Congresso de Métodos Numéricos em Engenharia 2015
Lisboa, 29 de Junho a 2 de Julho 2015

CRUSHING AND OEDOMETRIC DEFORMATION OF ROCKFILL USING DEM

João Manso[1*], João Marcelino[2] and Laura Caldeira[2]

1: Geotechnical Department
LNEC
Av. do Brasil 101, Lisbon
e-mail: jmanso@lnec.pt, web: http://www.lnec.pt

2: Geotechnical Department
LNEC
Av. do Brasil 101, Lisbon
e-mail: marcelino@lnec.pt,laurac@lnec.pt, web: http://www.lnec.pt

Keywords: Rockfill, *DEM*, particle breakage, crushing strength

Abstract. *The behavior of rockfill may be simulated using the discrete element (particle) modelling. Although its main advantage consists of not requiring the formulation of complex constitutive models, it requires extensive calibration to determine the particle–contact parameters in order to predict the macro-scale response. In this paper, the authors performed computer simulations of crushable agglomerates using distinct element method (DEM). These agglomerates were made by bonding elementary spheres using a stamp logic, in order to provide a statistical variability to the strength and shape of the agglomerates, similar to that of a real rockfill. This method was able to match the Weibull statistics of the crushing strength of real rockfill grains, when tested individually between parallel platens. Then, oedometric tests were simulated and compared quantitatively with the testing data. Several aspects were discussed, particularly, the effect of the loading rate on the position of the compression curves regarding the practical question of performing DEM simulations as fast as possible without creating inertia errors. They are also discussed in relation to characterising crushable rockfill during oedometric compression. These simulations of crushable agglomerates using DEM provides valuable insights concerning the micromechanical origins of rockfill compressibility. Once the model was calibrated through the results of tests performed, it can be used as a virtual laboratory to explore several aspects, as size and shape of the particle's sample. The model was capable of reproducing short-term compressibility (oedometer) tests, but the simulation of long-term compressibility and creep or secondary coefficient are still under development. The model also provided information on the evolution of the grain size distribution during loading of the specimen.*

1 INTRODUCTION

Rockfill material is widely used in many geotechnical engineering applications, such as rockfill dams and railroads, airports and railway embankments. Particularly, rockfill dams have been increasingly used due to their inherent flexibility, capacity to absorb large seismic energy, and adaptability to various foundation conditions. They also became an economical option since the increasing use of modern earth and rock moving equipment and locally available materials.

Several researchers [1–7] defined rockfill material as being composed of more than 50% coarse-grained soil larger than the No. 4 sieve size [8]. The Portuguese Guidelines for Dam Design [9] defined the upper limit of the particles size by construction issues, whereas the lower limit could be the size of clay. Nonetheless, the behaviour of compacted rockfill should not be influenced by the presence of smaller particles (less than 0,074 mm) and permeability should be greater than 10^{-5} m/s . By definition in [10], rockfill used in road embankments, should not have neither more than 30 % of material passing in *ASTM* sieve 1", nor more than 12 % of material passing *ASTM* sieve #200. Beyond that, the upper limit of the particle dimensions should be 2/3 of the height of each construction layer or 0,80 m. Therefore, within embankments, particles may cover a wide range of dimensions, from clayey materials to rockfill. In order to differentiate them, three categories are usually considered (Figure 1): soils, soil-rock mixtures and rockfill. In contrast to sand and gravel, rockfill grains are generally characterised by a lower crushing strength and experience higher contact forces due to their larger size and coarse gradation.

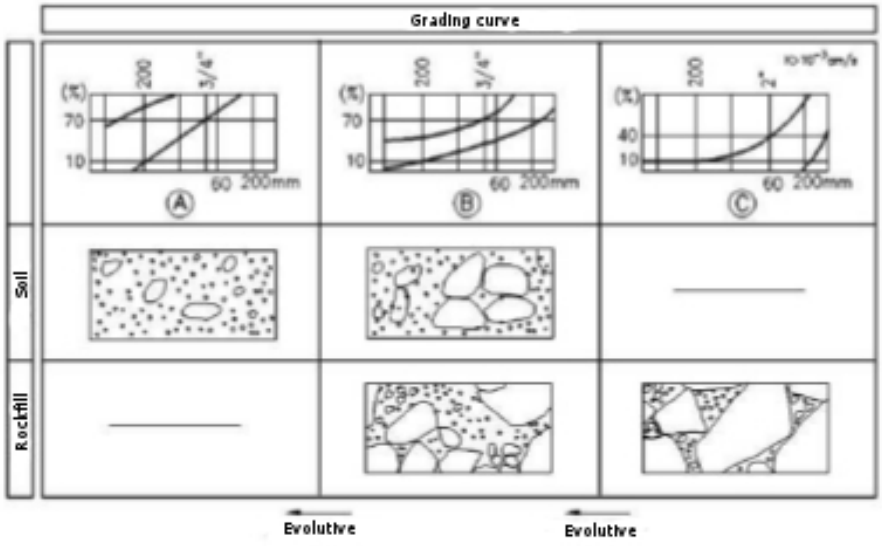

Figure 1: Typical grading curve for: a – soil, b – soil-rockfill mixtures and c – rockfill. Adapted from [11]

For a crushable rockfill material, particle breakage considerably influences its mechanical behaviour [1, 12–17]. Under compression or shear the crushing of particles modifies the grain size distribution, increasing the percentage of fine material [18]. Consequently, these differences in grain size distribution and in the available range of packing densities modifies the material permeability, its frictional properties and the critical states. Many researchers [12, 14, 15, 19, 20] experimentally investigated the role of particle breakage (large-scale triaxial tests, multiaxial tests, and true triaxial tests) in the mechanical behaviour of this type of geomaterials, characterising the influence of particle breakage in the strength of rockfill materials [1, 13, 19, 21–23]. In order to comprehensively represent the degree of particle breakage during loadings, several researchers proposed different breakage indexes, based on particle-size distributions before and after a test [1, 12, 14, 17, 24]. Miura et al. (2003) [25] defined the breakage factor during the consolidation and shearing process using increments of fines content (75 mm or smaller). Miura and O-Hara (1979) [26] considered the increase in the particle surface area to quantify the degree of particle crushing in the loading process. On the other hand, Einav (2007) [27] included a relative particle breakage index based on fractal theory and, relying in this work, Wood and Maeda (2008) [28] proposed a grading state index to quantify the degree of particle breakage. Consequently, some researchers developed elastoplastic models [29, 30], bounding surface models [31], and disturbed state concept models [19, 22] incorporating the breakage index in order to capture the stress-strain behaviours of crushable geomaterials.

Rockfill materials particle sizes range from a few millimetres to over a metre, commonly leading in rockfill dams to D_{50} sizes in the range 10–40 cm. Due to the large size particles of such granular aggregates, testing them under oedometric, direct shear or triaxial conditions would require equipment of impressive dimensions. The largest testing cells described in the literature [1, 32–35] were only capable of testing rockfill aggregates with maximum particle sizes not exceeding 15–20 cm [36]. A solution for this problem consists of reducing the size of the rockfill materials for testing using modelling techniques [19] (Figure 2a), such as: the scalping technique [37], parallel gradation technique [38], generation of quadratic grain-size distribution curve [39], and replacement technique [40]. Among these, Ramamurthy and Gupta (1986) [41] considered the parallel gradation method as the most appropriate. However, rockfill behaviour depends on its grain size scale, as shown by tests performed on materials with different mean grain size, but equivalent grain size distributions [1,32,33,36,42]. Particle breakage controls rockfill mechanical behaviour and is affected by scale effects, then, it is expected that scale effects are present in the constitutive behaviour of rockfill [36]. As it is almost impossible to test real size specimens, researchers studied alternative procedures to extrapolate results from a reduced scale to in situ conditions. Although it is useful to propose rules to scale some rockfill properties, such as strength [43], difficulties arise when considering other aspects of constitutive behaviour [36]. The discrete element method [44] can be an effective tool for investigating size effects, provided it is capable of properly simulate grain failure mechanisms for several stress paths [17, 45–51].

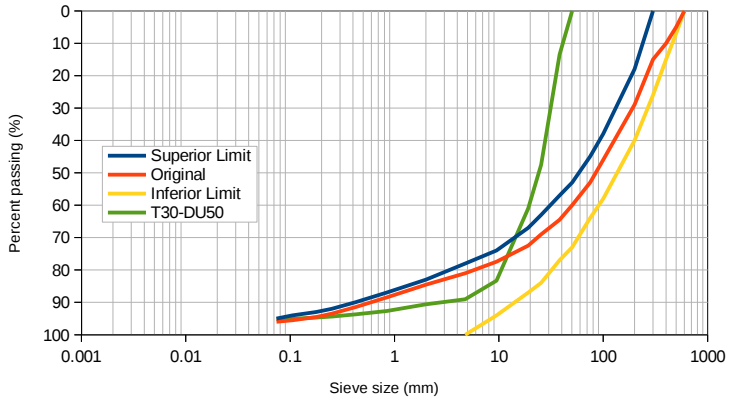

(a) Grading curves used in the beginning of the test

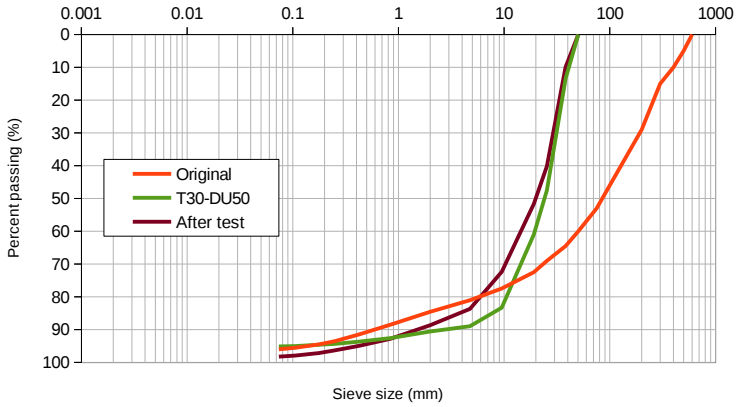

(b) Grading curve obtained after the test

Figure 2: Test grading curves

Several approaches were adopted to study particle breakage using *DEM*. Some considered subparticles joined by bonding or cohesive forces [45,52,53,53–56], another approach replaced a particle which verified a predefined failure criterion with an equivalent group of smaller particles [57–60]. These techniques were employed with either discs in 2D or spheres in 3D. When considering particles with general shapes, the technique consisted of bonding unbreakable and nondeformable subparticles creating a breakable particle. Then, if the bond between these subparticles broke, breakage occurred [61,62]. Other researchers proposed a method that combined finite element method (*FEM*) with discrete element implementations [20, 63]. In this method, particle movements and interactions

were determined using *DEM* ([64]) and the deformation of the rockfill material was solved computationally according to the rheological behaviour of the material, adopting a finite element mesh for each particle. A natural evolution of the *DEM*is to be capable of reproducing the complex mechanical behaviour of granular geomaterials, such as deformability and crushability, and to simulate accurately and conveniently the particle breakage phenomenon, despite the complexity of the considered particle shapes.
This paper deals with laboratory testing and discrete element modelling of rockfill materials collected from a dam site located in the north of Portugal. The model parameters were calibrated through results of tests performed on samples with a given grain size distribution. Then, the model allowed to study the influence of density and pressure on the strength and deformation of rockfill material through the loading steps of an oedometric compression test. This model and the basic mechanical behaviour of the material derived from Montesinho dam would be the same as that of rockfill materials at other sites. However, the strength and deformation of rockfill materials depend on the rock type and mineralogy and some of the material constants may be different for rockfill materials at other sites.

2 MODELLING OF A ROCKFILL PARTICLE

2.1 Contact constitutive models

The PFC^{2D} program [65] uses the distinct element method with the soft contact approach. This approach assumes that elements have a finite normal stiffness and allows bodies to overlap in order to represent elastic flattening at contacts. The constitutive representation of contact points between two elementary spheres include a stiffness model, a bonding model and a slip model. In the linear contact-stiffness model, the normal and shear tangent stiffness at a contact, K_n and K_s respectively, are computing assuming that those stiffnesses act in series, which can be written as:

$$K_n = \frac{k_n^A k_n^B}{k_n^A + k_n^B} \tag{1}$$

and

$$K_s = \frac{k_s^A k_s^B}{k_s^A + k_s^B} \tag{2}$$

where k_n^A and k_n^B represent the normal stiffness of two contacting objects A and B, and k_s^A and k_s^B represent the shear stiffnesses, expressed as the force per unit displacement.
The bonding model resembles a pair of elastic springs at a point of glue. It limits both normal and shear forces that a contact can carry by imposing bond-strength limits. When a bond is created between two spheres, the maximum shear force that it can sustain in tension is specified as well as the the maximum shear force it can bear before breaking. Note that these values may be modified at any time during the simulation. When one

of these values is exceeded, the bond breaks. This type of bond does not resist to a bending moment, due to the fact that it acts over a considerable small area of contact point. Therefore, if a third sphere does not exist to restrain the motion, it has no rolling resistance [45].
Finally, the slip model acts between two unbonded spheres in contact or after a bond breaks between two bonded spheres. It allows the contacting spheres to slip at a limiting shear force, governed by Coulomb's equation, and limits the shear force between them. When two spheres have different values of friction coefficients, the smaller one is used to calculate the maximum allowable shear force before sliding occurs:

$$F^s_{max} = \mu |F^n_i| \tag{3}$$

where F^s_{max} represents the maximum shear contact force, where μ is the coefficient of friction, and F^n_i represents the normal component of the contact force.

2.2 Variability implementation

The agglomerates intended to model rockfill particles should be capable of simulate the crushing strength of a real grain, due to diametral breakage of the bonded agglomerates between flat platens, and at the same time reproduce realistic Weibull distributions of crushing strength for a group of specimens. In order to achieve this, some considerations had to be made. Following [45], to avoid the effect of locked-in forces, that emerge from overlaps between spheres when creating a bond (which would release strain energy if the bond is broken), a sphere should be replaced by a group of agglomerates made from a regular assembly of spheres in hexagonal close packing (*HCP*), without initial overlap. The main purpose of this regular packing is to minimise the space between the spheres of the agglomerate [45,66]. Then, in order to provide a statistical variability to the strength and shape of the agglomerates, similar to that of a real rockfill, we introduced the stamp logic presented by [67], which is illustrated in Figure 3.
This logic creates a clump by stamping a circled area that corresponds to the desired grain size. The centre position of the particles that lie within this area are added to a clump and particles grouped in this way intend to represent a grain acting as a single particle. The clump size is defined by specifying the radius of the stamp circle with a standard deviation and clump stamping is continuously activated until all particles in the assembly belong to a clump (Figure 4b).

3 MODELLING OEDOMETRIC COMPRESSION OF A ROCKFILL SYSTEM

Each numerical test performed in this work started by create an initial set of *exo-spheres*, which consisted in placing them at random with a size slightly smaller than the required, without overlaps between themselves. Then, they were expanded to the final size and cycled until equilibrium was reached, reducing unwanted gaps. Following [45, 66] shear

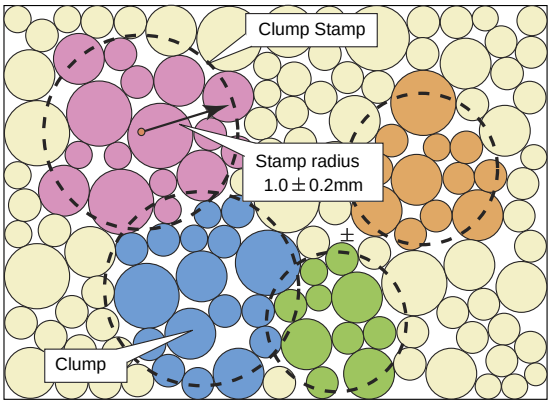

Figure 3: Illustration of stamping logic to control clump size [67]

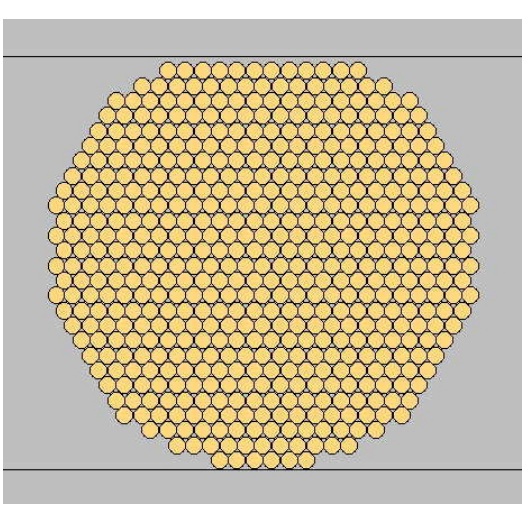

(a) Unclumped particle

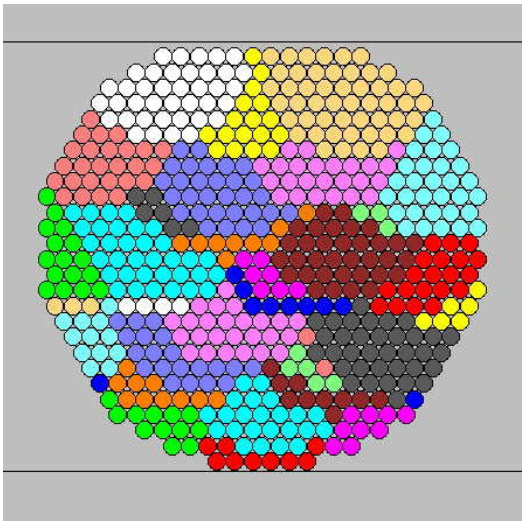

(b) Clumped particle

Figure 4: Introducing variability in a typical rockfill particle

stiffness and friction were reduced to zero, while lateral wall stiffness was reduced ten times the initial normal stiffness, which was increased 100-fold during the process of preparing the sample (Table 1). In order to insert the aggregates a linked list storing the coordinates of exo-spheres centres was created and then they were deleted. In their place, with the centre located at the list coordinates, were created aggregates, and applied the clump logic until all particles were clumped. After this, the new assembly was cycled until equilibrium was reached again, before starting the test. At this time, the shear and normal stiffnesses of the balls of the agglomerates were set to their final value ($3 \cdot 10^9$ N/m).
In order to reduce the possibility of bonds breaking during the preparation of the specimen,

Input parameter	Numerical value
Friction coefficient	0
Shear stiffness [N/m]	0
Normal stiffness [N/m]	$5 \cdot 10^{10}$
Wall stiffness [N/m]	$5 \cdot 10^{7}$

Table 1: Adopted properties for specimen preparation

their strengths were initially set very high ($1 \cdot 10^{9}$ Pa) until equilibrium was reached. This objective was achieved and no bonds broke during the sample preparation process, after introducing the clumps, for an equilibrium stress of 5 kPa. Finally, before starting the test, bond strengths were fixed to their final value ($1 \cdot 10^{6}$ Pa) and friction coefficient was set to 0.5, corresponding to a contact friction angle of 26.5 (Table 2).

Input parameter	Numerical value
Friction coefficient	0.5
Normal and shear stiffness [N/m]	$3 \cdot 10^{9}$
Normal and shear stiffness (parallel bonds) [N/m]	$3 \cdot 10^{9}$
Normal and shear strength (parallel bonds) [MPa]	$1 \cdot 10^{6}$

Table 2: Adopted properties for test modelling

Figure 5 shows the layout of particles used in this work. The characteristics of the model are presented in Table 3, which resulted in 1520 agglomerates. The model was then uniaxially compressed, in 100 kPa stages (until 1 MPa), by moving the top and bottom walls progressively together and fixing the position of the other pair of walls, to achieve the desired stress path. Following [45], the walls moved at a maximum speed of 0.01 m/s which were controlled by a servomechanism to reach the desired stress. This maximum speed was considered slow enough to eliminate rate effects, due to any bouncing that could occur initially for unloaded agglomerates. The *stress* was determined by summing and averaging all contact forces on the top wall. The voids ratio was calculated considering the solids volume as the total area of the circles, resulting in an initial value of 0.25.
Several velocity-limited loading tests were performed in order to check for possible inertia effects on the location of the virgin compression line. The limited velocities started with a value of 2 m/s and decreased until 0.01 m/s. It was considered that no dynamic effect occurred on the compression behaviour for platen velocities below 0.01 m/s (Figure 6b). However, when the velocities were allowed to reach higher values, an increase of the strength of individual agglomerates was registered, as seen in Figure 6a, which meant that grains would start crushing at a higher stress level. Furthermore, when analysing the numerical timestep at which bond breakage happened, they appeared for a smaller

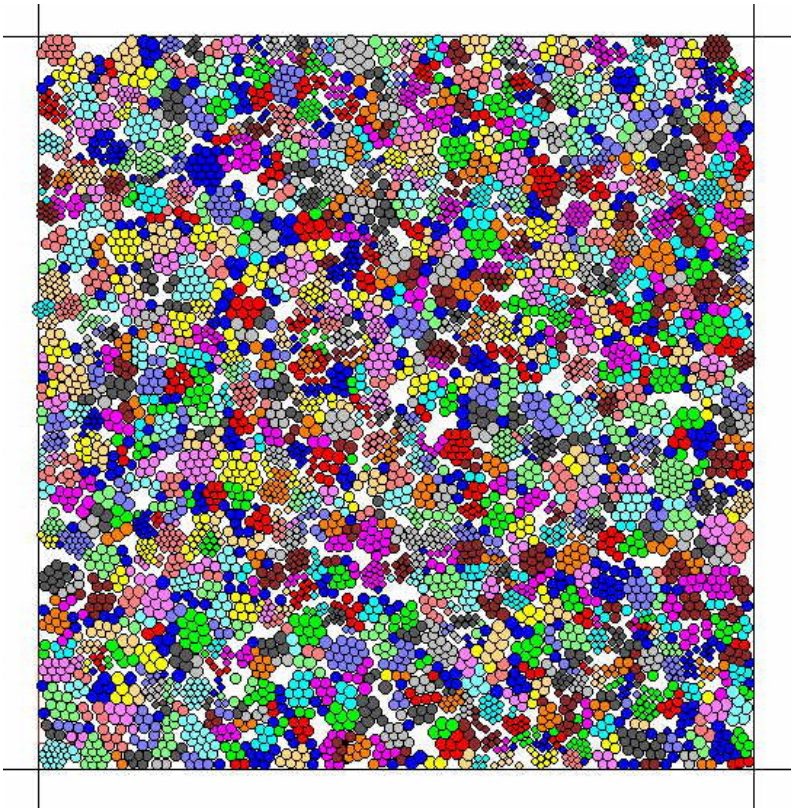

Figure 5: Rockfill specimen of 1520 agglomerates

Input parameter	Numerical value
Sample height [m]	0.474
Sample width [m]	0.500
R_{min} [mm]	0.0095
R_{max} [mm]	0.0191
Clump size [mm]	1.0 ± 0.2
Density $[kg/m^3]$	2052

Table 3: Agglomerate characteristics adopted to model a typical rockfillparticles

timestep in the case of higher compression rates (Figure 7). The resulting behaviour was, as observed in Figure 6b, equivalent, leading to a similar amount of bond breakage.
Since the beginning of the oedometric test irrecoverable compression was registered, which happened beyond 100 kPa. This occurred without any significant breakage, so this behaviour can be attributed to agglomerates rearrangement due to elastic compression. The breakage started at approximately 400 kPa (for a limiting velocity of 0.01 m/s) and 600 kPa (for a limiting velocity of 0.5 up to 2 m/s).

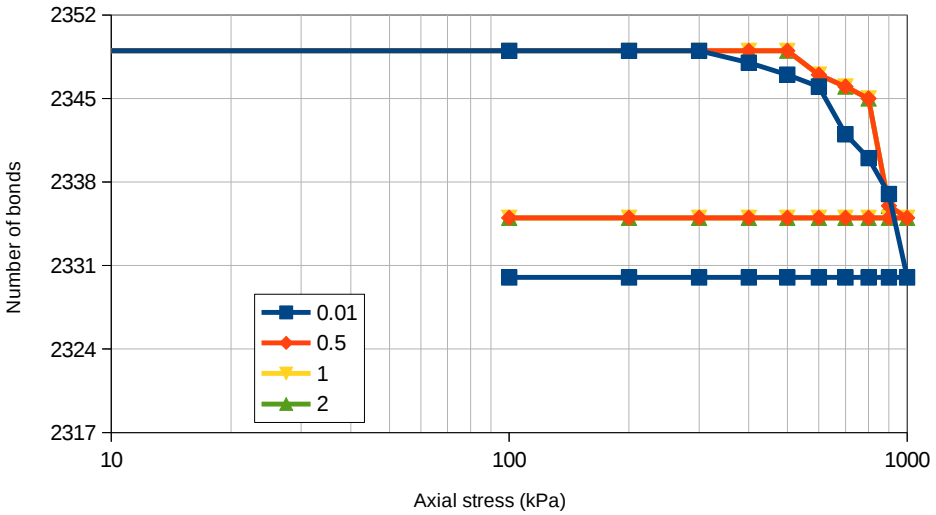

(a) Numerical timesteps against bond breakage

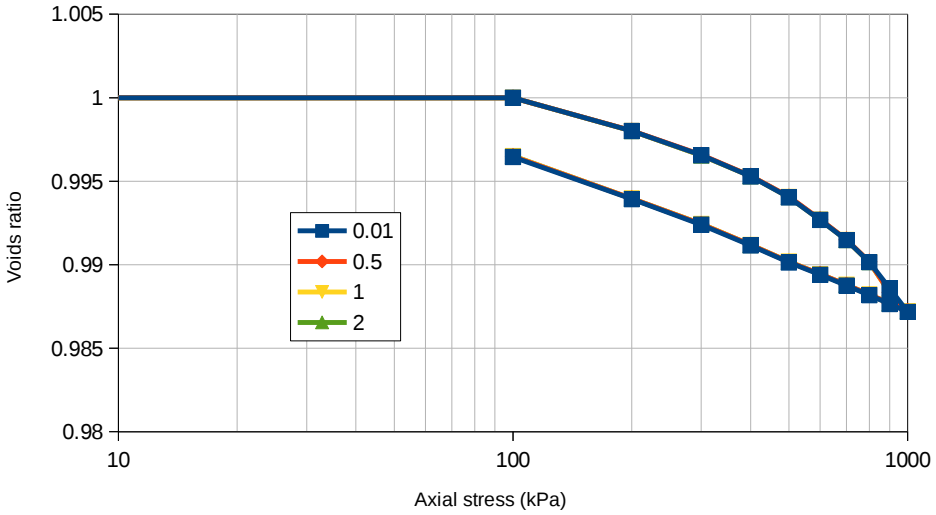

(b) Voids ratio against axial stress

Figure 6: Effect of limiting compression rate on oedometric compression curve

Nakata et al. (2001) [68] compared the results of single-particle crushing tests with the one-dimensional compression of samples of the same uniformly graded sand. The results showed that the macroscopic stress level required to cause crushing and irrecoverable compression in a sand sample, was much smaller than that required to break individual grains. They attributed this to the unequal distribution of internal contact forces within

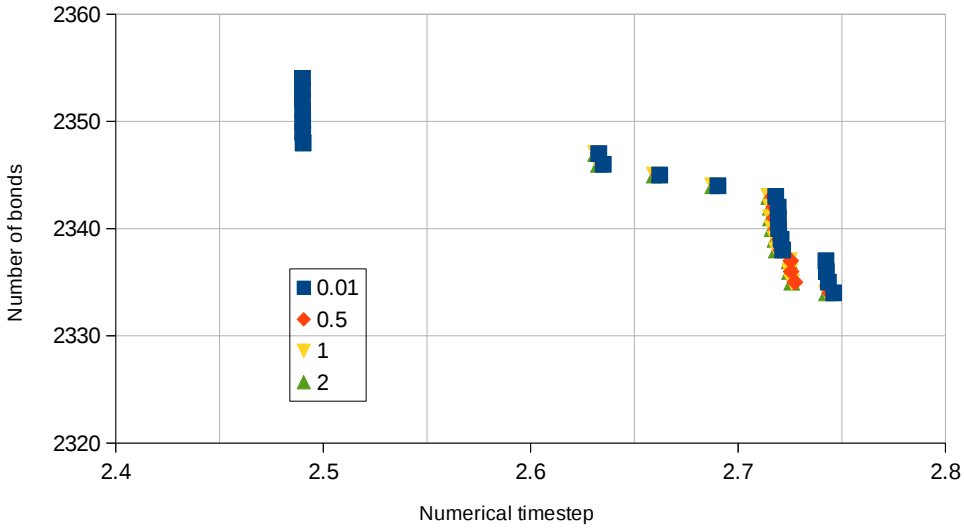

Figure 7: Numerical timesteps against bond breakage

an aggregate of grains. Cundall and Strack (1979) [44] found that only a number of heavily loaded chains of particles respond to an externally applied stress, which had been observed experimentally by Oda and Konishi (1974) [69]. Whereas, the remaining particles within the mass are only slightly loaded [70]. Their main contribution to the system is the stabilisation of the main loading chains. As a result of this particle breakage, several authors [71–74] have studied diametrically loaded single particles. Cheng et al. (2001) [71] described two breakage phases: an initial one, governing the beginning of individual grains breakage, and a second one in which further breakage continued as the compression proceeded. In a rockfill sample, agglomerates are supported by nearby agglomerates, increasing its coordination number. This aspect should distribute stresses along its contacts, leading to a reduction in tensile stress, when compared to single particle crushing tests [45, 75]. Therefore, an agglomerate in a rockfill sample might break at an applied stress even higher than the crushing strength.

As in the work of Cheng et al. (2003) [45] regarding a soil sample, there is an interesting coincidence between the beginning of linear bond breakage plot against the logarithm of mean stress and when rockfill reaches the linear logarithmic compression line at approximately 600 kPa, which is clearer for a limited velocity of 0.01 m/s. This macro behaviour of the simulated rockfill can be referred as clastic yielding and happens when the applied stress causes the onset of particle crushing, assuming that the onset of particle breakage leads to the bend of the normal compression line, causing the rapid increase of the material compressibility index [76]. During unloading (swelling curve) the simulated rockfill element showed an elastic behaviour and no bond breakage occurred.

Figure 8 compares isotropic compression curves between the rockfill sample and the *DEM*

simulation with a platen speed of 0.01 m/s. Both shapes are similar and the *DEM* simulation captures the transition from particle rearrangement, due to elastic compression, into what may be described as clastic compression. We are aware that due to the nature of the real material, there are greater variability in the real rockfill. Comparing rockfill particles with the agglomerates in the *DEM* simulation, it is clear that there is a greater variety of sizes and asperities in the real material and that agglomerates have only a limited number of component spheres [45]. These particularities may explain the differences between the isotropic compression line, specially concerning creep that appears in the material at the end every load step and it is not reflected numerically (Figure 8 and 9). The rockfill sample continues fragmenting at constant loads, whereas the simulated rockfill remains stable when the increase of load stops. This can be also attributed to the linear contact-stiffness adopted and could be a matter of selecting a different one that considered decrease of strength with time. Some researchers [77] suggested that in order to improve numerical results, the agglomerates should be modelled using spheres with dimensions close to the comminution limit of silica sands, but this has for now unrealistic computation costs.

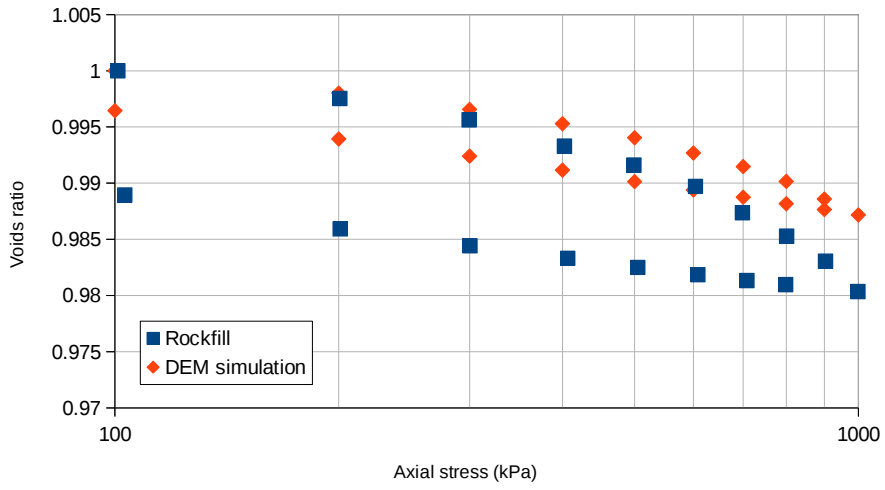

Figure 8: Normalised oedometric compression curves

4 CONCLUSIONS

Short-term compressibility on rockfill behaviour (oedometer tests) was successfully approached through *DEM* modelling provided a careful specimen preparation in the model and defining the parameters based on laboratory test results.

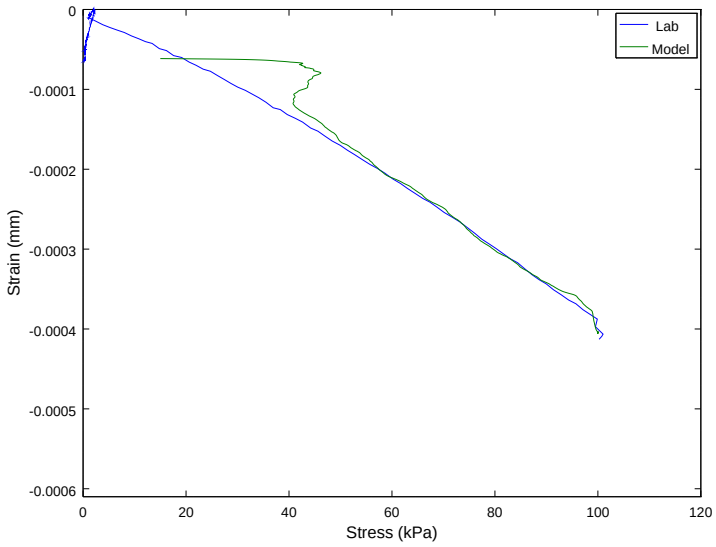

(a) 100 kPa

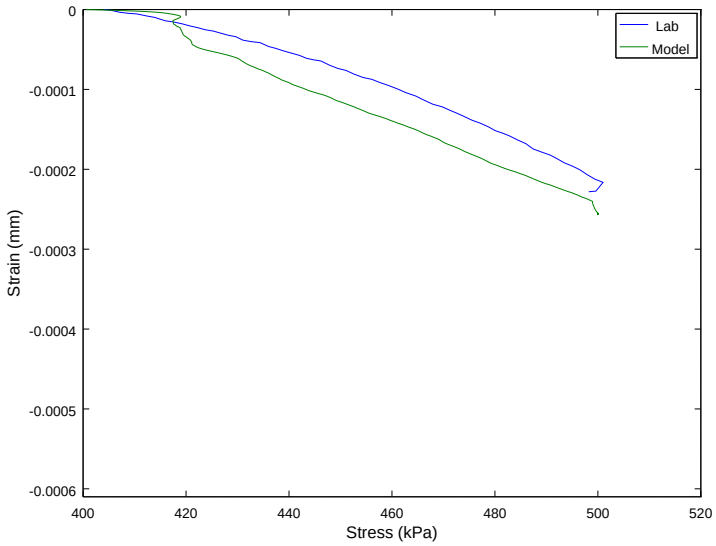

(b) 500 kPa

Figure 9: Oedometric test stress strain curves

The developed model adopted the clump logic to simulate rockfill particles allowing them to randomly subdivide into smaller shapes. This has been achieved by introducing the idea that a rockfill grain can be considered to be an agglomerate of bonded micro-elements, here represented as clumps. Breakage occurred in the specimen when a bond between subparticles broke. This approach seemed to be capable of creating a lifelike distribution of grain crushing strengths and rockfill compressibility behaviour.
Several test simulations were conducted limiting wall velocities up to 2 m/s in order to perform *DEM* simulations as fast as possible without creating inertia errors.
In further developments, the simulation of long-term compressibility and creep or secondary coefficient may be achieved by including a particle breakage criterion, which incorporates the mechanics of crack propagation in brittle materials. Furthermore, models will be developed in order to simulate triaxial tests with different stress paths and be capable of replicating the mechanical behaviour of rockfill, particularly its strength, dilatancy, and critical states. Special attention will be given to the evolution of the grain size distribution during loading of specimens for a wide range of particle sizes. This study on the micromechanics of granular interactions should lead to improved continuum rockfill models.

REFERENCES

[1] R. J. Marsal, Large-Scale Testing of Rockfill Materials, Journal of the Soil Mechanics and Foundation Division, ASCE 93 (2) (1967) 27–43.

[2] T. M. Leps, Review of shearing strength of rockfill., J. Soil Mech. and Found. Div. 4 (96) (1970) 1159–1170.

[3] N. D. Marschi, C. K. Chan, H. B. Seed, Evalution of properties of rockfill materials., J. Soil Mech. and Found. Div. 1 (98) (1972) 95–114.

[4] J. A. Charles, K. S. Watts, The influence of confining pressure on the shear strength of compacted rockfill., Geotechnique 4 (30) (1980) 353–367.

[5] N. Barton, B. Kjaernsli, Shear strength of rockfill., J. Geotech. Engrg. Div. 7 (107) (1981) 873–891.

[6] G. M. Matheson, Relationship between compacted rockfill density and gradation., Journal of Geotechnical Engineering 112 (12) (1987) 1119–1124.

[7] Y. Xiao, H. Liu, Y. Chen, J. Jiang, Strength and Deformation of Rockfill Material Based on Large-Scale Triaxial Compression Tests.I: Influences of Density and Pressure, Journal of Geotechnical and Geoenvironmental Engineering (2014) 04014070doi:10.1061/(ASCE)GT.1943-5606.0001176.

[8] ASTM, Standard practice for classification of soils for engineering purposes (Unified Soil Classification System), Tech. rep. (2006).

[9] Normas de projecto de barragens. (1993).

[10] S. A. Estradas de Portugal, Caderno de encargos tipo obra - Estradas de Portugal, S. A., Tech. rep. (2009).

[11] E. Maranha das Neves, Fills and embankments, in: International Conference on Geotechnical Engineering of Hard Soils and Soft Rocks, General Report, Athens, v.3, 1993, pp. 2023–2037.

[12] B. O. Hardin, Crushing of soil particles, Journal of Geotechnical and Engineering, ASCE 111 (10) (1985) 1177–1192.

[13] B. Indraratna, a. S. Balasubramaniam, L. S. S. Wijewardena, Large-scale triaxial testing of greywacke rockfill, Géotechnique 44 (3) (1993) 539–543. doi:10.1680/geot.1994.44.3.539.

[14] P. Lade, J. Yamamuro, P. Bopp, Significance of particle crushing in granular materials, Journal of Geotechnical Engineering 122 (4) (1996) 309–316.

[15] G. R. McDowell, M. D. Bolton, D. Robertson, The fractal crushing of granular materials, Journal of the Mechanics and Physics of Solids 44 (12) (1996) 2079–2102.

[16] I. Einav, Breakage mechanicsPart II: Modelling granular materials, Journal of the Mechanics and Physics of Solids 55 (6) (2007) 1298–1320. doi:10.1016/j.jmps.2006.11.004.
URL http://linkinghub.elsevier.com/retrieve/pii/S0022509606001839

[17] Y. Xiao, H. Liu, Y. Chen, J. Jiang, Strength and Deformation of Rockfill Material Based on Large-Scale Triaxial Compression Tests.II: Influence of Particle Breakage, Journal of Geotechnical and Geoenvironmental Engineering (2014) 04014071doi:10.1061/(ASCE)GT.1943-5606.0001177.

[18] F. Casini, G. M. B. Viggiani, S. M. Springman, Breakage of an artificial crushable material under loading, Granular Matter 15 (5) (2013) 661–673. doi:10.1007/s10035-013-0432-x.

[19] A. Varadarajan, K. G. Sharma, K. Venkatachalam, A. K. Gupta, Testing and Modeling Two Rockfill Materials, Journal of Geotechnical and Geoenvironmental Engineering 129 (3) (2003) 206–218.

[20] G. Ma, W. Zhou, X. L. Chang, Modeling the particle breakage of rockfill materials with the cohesive crack model, Computers and Geotechnics 61 (2014) 1320–1143. doi:10.1016/j.compgeo.2014.05.006.
URL http://dx.doi.org/10.1016/j.compgeo.2014.05.006

[21] B. Indraratna, D. Ionescu, H. D. Christie, Shear Behaviour of Railway Ballast based on Large Scale Triaxial Testing, Journal of Geotechnical and Geoenvironmental Engineering 124 (5) (1998) 439–449.

[22] A. Varadarajan, K. Sharma, S. Abbas, A. Dhawan, Constitutive Model for Rockfill Materials and Determination of Material Constants, International Journal of Geomechanics 6 (4) (2006) 226–237. doi:10.1061/(ASCE)1532-3641(2006)6:4(226).
URL http://link.aip.org/link/IJGNAI/v6/i4/p226/s1&Agg=doi

[23] A. K. Gupta, Effect of particle size and confining pressure on breakage and strength parameters of rockfill materials, Electronic Journal of Geotechnical Engineering 14 H.

[24] K. Lee, I. Farhoomand, Compressibility and crushing of granular soil in anisotropic triaxial compression, Canadian Geotechnical Journal IV (1).

[25] S. Miura, Y. Kazuyoshi, T. Asonuma, Deformation-strength evaluation of crushable volcanic soils by laboratory and in-situ testing, Soils and Foundations 43 (4) (2003) 47–57. doi:10.1248/cpb.37.3229.

[26] N. Miura, S. O-Hara, Particle-crushing of a decomposed granite soil under shear stresses., Soils and Foundations 19 (3) (1979) 1–14. doi:10.3208/sandf1972.19.3_1.

[27] I. Einav, Breakage mechanics - Part I: Theory, Journal of the Mechanics and Physics of Solids 55 (6) (2007) 1274–1297. doi:10.1016/j.jmps.2006.11.003.
URL http://linkinghub.elsevier.com/retrieve/pii/S0022509606001827

[28] D. M. Wood, K. Maeda, Changing grading of soil: Effect on critical states, Acta Geotechnica 3 (1) (2008) 3–14. doi:10.1007/s11440-007-0041-0.

[29] W. Salim, B. Indraratna, A new elastoplastic constitutive model for coarse granular aggregates incorporating particle breakage, Canadian Geotechnical Journal 41 (4) (2004) 657–671. doi:10.1139/t04-025.

[30] A. Daouadji, P. Hicher, An enhanced constitutive model for crushable granular materials., International Journal for Numerical and Analytical Methods in Geomechanics 34 (6) (2009) 555–580. doi:10.1002/nag.

[31] A. R. Russell, N. Khalili, A bounding surface plasticity model for sands exhibiting particle crushing, Canadian Geotechnical Journal 41 (6) (2004) 1179–1192. doi:10.1139/t04-065.

[32] R. J. Marsal, Mechanical properties of rockfill, in: R. C. Hirschfeld, S. J. Poulos (Eds.), Embankment-dam engineering: Casagrande volume, john wiley Edition, 1973, pp. 109–200.

[33] N. D. Marachi, C. K. Chan, H. B. Seed, J. M. Duncan, Strength and deformation characteristics of rockfill materials., Tech. rep., University of California, Berkeley, CA, Report TE-69-5. (1969).

[34] N. D. Marachi, C. K. Chan, H. B. Seed, Evaluation of properties of rockfill materials, Soil Mech. Found. Eng. Div. ASCE 98 (1) (1972) 95–114.

[35] E. S. Nobari, J. M. Duncan, Effect of reservoir filling on stresses and movements in earth an rockfill dams, Tech. rep., Department of Civil Engineering, Report n. TE-72-1. University of California (1972).

[36] E. E. Alonso, M. Tapias, J. Gili, Scale effects in rockfill behaviour, Géotechnique Letters 2 (July-September) (2012) 155–160. doi:10.1680/geolett.12.00025.

[37] J. Zeller, R. Wullimann, The shear strength of the shell materials for the Go-Schenenalp Dam, Switzerland., in: 4th Inst. J. on SMFE, London, UK, 1957, pp. 399–404.

[38] J. Lowe, Shear strength of coarse embankment dam materials., in: 8th Int. Congress on Large Dams, 1964, pp. 745–761.

[39] E. Fumagalli, Tests on cohesionless materials for rockfill dams., Journal of Soil Mechanics & Foundations Division 95 (1) (1969) 313–332.

[40] R. Frost, Some testing experiences and characteristics of boulder-gravel fills in earth dams., in: Evaluation of relative denisty and its role in geotechnical projects involving cohesionless soils., 1973, pp. 207–233.

[41] T. Ramamurthy, K. Gupta, Response paper to how ought one to determine soil parameters to be used in the design of earth and rockfill dams., in: Indian Geotechnical Conf., New Delhi, 1986, pp. 15–19.

[42] E. Alonso, N. Pinyol, S. Olivella, A review of Beliche Dam, Géotechnique 55 (4) (2005) 267–285. doi:10.1680/geot.2005.55.4.267.
URL http://www.icevirtuallibrary.com/content/article/10.1680/geot.2005.55.4.267

[43] E. Frossard, W. Hu, C. Dano, P. Y. Hicher, Rockfill shear strength evaluation: a rational method based on size effects., Geotechnique 62 (5) (2012) 415–427.

[44] P. Cundall, O. Strack, A discrete numerical model for granular assemblies, Geotechnique 29 (1) (1979) 47–65.
URL http://www.icevirtuallibrary.com/content/article/10.1680/geot.1979.29.1.47

[45] Y. Cheng, Y. Nakata, M. Bolton, Discrete element simulation of crushable soil, Géotechnique 53 (7) (2003) 633–641. doi:10.1680/geot.2003.53.7.633.
URL http://www.icevirtuallibrary.com/content/article/10.1680/geot.2003.53.7.633

[46] Y. Cheng, M. Bolton, Y. Nakata, Crushing and plastic deformation of soils simulated using DEM, Geotechnique 54 (2) (2004) 131–141.

[47] S. Lobo-Guerrero, L. E. Vallejo, Discrete Element Method Analysis of Railtrack Ballast Degradation during Cyclic Loading, Granular Matter 8 (3-4) (2006) 195–204. doi:10.1007/s10035-006-0006-2.
URL http://link.springer.com/10.1007/s10035-006-0006-2

[48] S. Lobo-Guerrero, L. E. Vallejo, L. F. Vesga, Visualization of Crushing Evolution in Granular Materials under Compression Using DEM, International Journal of Geomechanics 6 (3) (2006) 195–200. doi:10.1061/(ASCE)1532-3641(2006)6:3(195).

[49] S. Lobo-Guerrero, L. E. Vallejo, Analysis of crushing of granular material under isotropic and biaxial stress conditions., Soils and Foundations 45 (4) (2006) 79–87.

[50] J. Wang, H. Yan, DEM analysis of energy dissipation in crushable soils, Soils and Foundations 52 (4) (2012) 644–657. doi:10.1016/j.sandf.2012.07.006.
URL http://dx.doi.org/10.1016/j.sandf.2012.07.006

[51] A. Lashkari, A. Golchin, On the influence of elastic-plastic coupling on sands response, Computers and Geotechnics 55 (2014) 352–364. doi:10.1016/j.compgeo.2013.09.016.
URL http://dx.doi.org/10.1016/j.compgeo.2013.09.016

[52] R. Jensen, M. Plesha, T. Edil, P. Bosscher, N. Kahla, DEM Simulation of Particle Damage in Granular Media - Structure Interfaces, The International Journal of Geomechanics 1 (1) (2001) 21–39. doi:10.1061/(ASCE)1532-3641(2001)1.

[53] O. Harireche, G. R. McDowell, Discrete element modelling of cyclic loading of crushable aggreates, Granular Matter 5 (3) (2003) 147–151. doi:10.1007/s10035-003-0143-9.

[54] M. Bolton, Y. Nakata, Y. Cheng, Micro- and macro-mechanical behaviour of DEM crushable materials 3 (6) (2008) 471–480. doi:10.1680/geot.2008.58.6.471.
URL http://discovery.ucl.ac.uk/126472/

[55] S. Levasseur, Y. Malécot, M. Boulon, E. Flavigny, Y. Malecot, On the role of particle breakage in the shear failure behavior of granular soils by DEM, International Journal for Numerical and Analytical Methods in Geomechanics 37 (2013) 832–854. doi:10.1002/nag.

[56] E. Alaei, A. Mahboubi, A discrete model for simulating shear strength and deformation behaviour of rockfill material, considering the particle breakage phenomenon, Granular Matter 14 (6) (2012) 707–717. doi:10.1007/s10035-012-0367-7.
URL http://link.springer.com/10.1007/s10035-012-0367-7

[57] O. Tsoungui, D. Vallet, J.-c. Charmet, Numerical model of crushing of grains inside two-dimensional granular materials, Powder Technology 105 (1-3) (1999) 190–198.

[58] S. Lobo-Guerrero, L. E. Vallejo, Discrete Element Method Evaluation of Granular Crushing Under Direct Shear Test Conditions, Journal of Geotechnical and Geoenvironmental Engineering 131 (10) (2005) 1295–1300. doi:10.1061/(ASCE)1090-0241(2005)131:10(1295).

[59] T. Brosh, H. Kalman, A. Levy, Fragments spawning and interaction models for DEM breakage simulation, Granular Matter 13 (6) (2011) 765–776. doi:10.1007/s10035-011-0286-z.

[60] J. Bruchmüller, B. G. M. van Wachem, S. Gu, K. H. Luo, Modelling discrete fragmentation of brittle particles, Powder Technology 208 (3) (2011) 731–739. doi:10.1016/j.powtec.2011.01.017.

[61] E. Seyedi Hosseininia, a. a. Mirghasemi, Numerical simulation of breakage of two-dimensional polygon-shaped particles using discrete element method, Powder Technology 166 (2) (2006) 100–112. doi:10.1016/j.powtec.2006.05.006.

[62] S. a. Galindo-Torres, D. M. Pedroso, D. J. Williams, L. Li, Breaking processes in three-dimensional bonded granular materials with general shapes, Computer Physics Communications 183 (2) (2012) 266–277. doi:10.1016/j.cpc.2011.10.001.

[63] a. Munjiza, D. Owen, N. Bicanic, A combined finite-discrete element method in transient dynamics of fracturing solids, Engineering Computations 12 (2) (1995) 145–174. doi:10.1108/02644409510799532.

[64] A. Munjiza, The Combined Finite-Discrete Element Method, 2004. doi:10.1002/0470020180.

[65] I. C. G. Inc., PFC3D (Particle Flow Code in 3 Dimensions). Version 3.10. User manual. (2005).

[66] D. Robertson, Computer simulations of crushable aggregates., Ph.D. thesis, Cambridge University (2000).

[67] N. Cho, C. D. Martin, D. C. Sego, A clumped particle model for rock, International Journal of Rock Mechanics and Mining Sciences 44 (7) (2007) 997–1010. doi:10.1016/j.ijrmms.2007.02.002.
URL http://linkinghub.elsevier.com/retrieve/pii/S1365160907000172

[68] Y. Nakata, Y. Kato, M. Hyodo, A. Hyde, H. Murata, One-dimensional compression behaviour of uniformly graded sand related to single particle crushing strength, Soils and foundations 41 (2) (2001) 39–51.

[69] M. Oda, J. Konishi, Microscopic deformation mechanism of granular material in simple shear., Soils and Foundations 14 (4) (1974) 25–38. doi:10.1248/cpb.37.3229.

[70] J. Maranha, Discrete element modelling of rockfill behaviour. Collapse settlement., in: F. et. al (Ed.), Applications of Computational Mechanics in Geotechnical Engineering, Swets & Zeitlinger, Lisse, 2001.

[71] Y. Cheng, D. White, E. Bowman, M. D. Bolton, K. Soga, The observation of soil microstructure under load, in: 4th ICMGM, Powders and Grains, 2001, pp. 69–72.

[72] R. Deluzarche, B. Cambou, Discrete numerical modelling of rockfill dams, International Journal for Numerical and Analytical Methods in Geomechanics (June) (2006) 1075–1096. doi:10.1002/nag.

[73] L. Oldecop, E. Alonso, Theoretical investigation of the time-dependent behaviour of rockfill, Géotechnique 57 (3) (2007) 289–301. doi:10.1680/geot.2007.57.3.289.
URL http://www.icevirtuallibrary.com/content/article/10.1680/geot.2007.57.3.289

[74] T. Tran, R. Vénier, B. Cambou, Discrete modelling of rock-ageing in rockfill dams, Computers and Geotechnics 36 (1-2) (2009) 264–275. doi:10.1016/j.compgeo.2008.01.005.
URL http://linkinghub.elsevier.com/retrieve/pii/S0266352X08000062

[75] G. McDowell, M. D. Bolton, On the micromechanics of crushable aggregates, Geotechnique 48 (5) (1998) 667–679.
URL http://cat.inist.fr/?aModele=afficheN&cpsidt=2436386

[76] L. Oldecop, E. Alonso, Suction effects on rockfill compressibility, Geotechnique 53 (2) (2003) 289–292.

[77] K. Kendall, The impossibility of comminuting small particles by compression., Nature 272 (1978) 710–711.